Increased ice loading in the Antarctic Peninsula since the 1850s and its effect on Glacial Isostatic Adjustment

Grace A. Nield[1]*, Pippa L. Whitehouse[2], Matt A. King[1], Peter J. Clarke[1], Michael J. Bentley[2]

[1]School of Civil Engineering and Geosciences, Newcastle University, Newcastle upon Tyne, UK;

[2]Department of Geography, Durham University, Durham, UK

*Corresponding author; e-mail: g.a.nield@newcastle.ac.uk

Abstract. Antarctic Peninsula (AP) ice core records indicate significant accumulation increase since 1855, and any resultant ice mass increase has the potential to contribute substantially to present-day Glacial Isostatic Adjustment (GIA). We derive empirical orthogonal functions from climate model output to infer typical spatial patterns of accumulation over the AP and, by combining with ice core records, estimate annual accumulation for the period 1855-2010. In response to this accumulation history, high resolution ice-sheet modeling predicts ice thickness increases of up to 45 m, with the greatest thickening in the northern and western AP. Whilst this thickening is predicted to affect GRACE estimates by no more than 6.2 Gt/yr, it may contribute up to -7 mm/yr to the present-day GIA uplift rate, depending on the chosen Earth model, with a strong east-west gradient across the AP. Its consideration is therefore critical to the interpretation of observed GPS velocities in the AP.

1. Introduction

Antarctica is undergoing Glacial Isostatic Adjustment (GIA) in response to ice mass changes since the Last Glacial Maximum (LGM); however, the long-term rate and spatial pattern of GIA may have been significantly altered due to very recent (i.e. Late Holocene) changes in ice sheet mass balance. GIA models of Antarctica remain poorly constrained due to a dearth of available data and poor knowledge of Earth parameters and ice history [*Whitehouse et al.*, 2012a],

Geophys. Res. Lett., 39, L17504, doi:10.1029/2012GL052559.

particularly relating to the last few thousand years. Any significant load changes during this period will have a dominant effect upon the observed uplift rate in low viscosity regions, such as the Antarctic Peninsula (AP) [*Ivins et al.*, 2000].

In the AP, ice core records suggest an increase in annual accumulation since the 1850s, e.g. the Gomez ice core in Palmer Land (see Figure 1a) indicates a doubling of accumulation during this period [*Thomas et al.*, 2008]. Other ice cores [e.g., *Peel*, 1992] indicate that increases also occur elsewhere but the rate and magnitude is not uniform across the AP, with more increase seen in the west and north than in the east. This spatial pattern reflects the different climate conditions which prevail either side of the mountain chain which forms the spine of the AP, with warmer conditions on the western side resulting in more precipitation than on the colder, drier eastern side [*Miles et al.*, 2008].

We hypothesize that recent accumulation along the AP causes a viscoelastic response of sufficient magnitude that the resulting subsidence could be observed at the surface. This would counteract the predicted uplift due to deglaciation since the LGM, potentially explaining the low rates of present-day uplift observed by GPS [*Bevis et al.*, 2009; *Thomas et al.*, 2011]. This accumulation-related mass increase has not been included in recently reconstructed AP loading histories [e.g., *Ivins et al.*, 2011]. In this study, we examine the magnitude and spatial pattern of increasing accumulation over the AP since 1855 using evidence from several AP ice cores. We show the effect of the resulting ice-mass change upon present-day GIA uplift rates and investigate the impact on GRACE-derived rates of present-day ice-mass change.

2. Accumulation Data

We used an empirical orthogonal function (EOF) technique to estimate the spatial pattern of accumulation from the regional climate model RACMO2.1/ANT over the period 1989–2010 at 27 km resolution [*Lenaerts et al.*, 2012]. EOF analysis is commonly used in climate studies to identify statistically significant patterns in data and as a basis for temporal extrapolation [e.g., *Church et al.*, 2004]. Assuming that the spatial patterns of accumulation have remained the same over the last 155 years, the leading five EOFs (explaining around 99% of the 1989–2010 variance) were combined with data from five ice cores (locations shown in Figure 1a) [*Mosley-Thompson*, 1992; *Peel*, 1992; *Thomas et al.*, 2008] to estimate the accumulation history of the AP between 1855 and 2010. We identified an error in the published position of the Gomez ice core (shifting it to 73.99°S, 70.61°W; Figure 1a), and we used an updated accumulation time series which includes a field-based strain rate correction (pers. comm., E. Thomas, 2012).

Although the ice-core records terminate prior to 2010, we estimated annual accumulation up to 2010 by linearly extrapolating each record using the same rate of change as is observed between 1930 and the end of the ice-core record. This period was chosen because 1930 marks the onset of annual accumulation increase in the Gomez record [*Thomas et al.*, 2008], and based on the available data it is reasonable to assume that this increase continues beyond the end of the record. The method is considered conservative because the extrapolated rates lie well within the full range of gradients represented in each ice-core record. A sensitivity study was carried out varying the extrapolated rates by ±50% and it was found that this made no more than ±0.2 mm/yr difference to the predicted GIA uplift rates; this issue is therefore not considered further.

To evaluate how well the EOFs are able to reproduce observations, the reconstructed accumulation history for each ice-core location is plotted with the original ice-core data in Figure 1a. To confirm that the method is robust, the reconstruction was recomputed, omitting each ice core in turn, so that only data from the other four ice cores were combined with the EOFs. Figure 1b indicates that Gomez, Dyer Plateau and Dolleman Island ice-core data can be well reproduced using the EOF technique. The ~30 yr oscillation at James Ross Island is not well reproduced; however, the general trend, which is most important for our study, is robust. The trend at Siple Station is also not well reproduced; however, as this ice core lies at the southern extremity of our study domain and does not show the same accumulation increase as those in the northern AP, it will have minimal effect on the resulting predictions of ice thickness change. The misfits in these reconstructions are likely a combination of the ice cores not being representative of the wider area and/or the EOFs not representing the accumulation pattern well in those areas.

3. Ice-sheet Modeling

Following an increase in accumulation, an ice sheet will move towards a new equilibrium state by increasing its discharge rate, partially mitigating the loading effect of the accumulation increase. To examine this process, the reconstructed accumulation history was used to drive a high resolution (5 km) ice-sheet model (Glimmer community ice-sheet model, [*Rutt et al.*, 2009]) and predict changes in ice thickness. The model was set up with initial conditions of present-day bedrock elevation, ice thickness, and surface temperature [*Le Brocq et al.*, 2010], and run for several thousand years to an equilibrium state using the first year of the reconstructed accumulation history before being forced with the remaining accumulation history. Running the model to an initial equilibrium state isolates the effects of the accumulation changes on ice thickness between 1855 and 2010. The model domain was truncated at an ice divide at the southern end of the Peninsula (Figure 2). We prescribed zero ice flow across this boundary, similar to the method adopted by *Le Brocq et al.* [2011] when modeling the Weddell Sea embayment.

Total ice thickness was output every five time steps (i.e. every five years) during the model run and differenced with the initial equilibrium ice thickness to obtain the cumulative ice thickness change due to the reconstructed accumulation history. The ice-sheet model predicts ice thickness increases of up to 45 m over 155 years, with the greatest increases seen in the west and north of the AP (Figure 2a).

The importance of using an ice-sheet model is demonstrated by examining the difference (Figure 2c) between the ice thickness increase predicted from ice-sheet modeling (Figure 2a) and the sum of the reconstructed accumulation history (Figure 2b). Much of the accumulation increase over the narrow northern AP is offset by ice discharge into the ocean during the experiment, due to high velocity ice flow, reducing peak accumulation from 120 m to 45 m. At most other locations, where flow is slower, the difference between the summed accumulation history and ice-sheet model output is less than 10 m.

4. GIA Modeling

The output of the ice-sheet modeling was used to drive a GIA model and calculate the ongoing response of the solid Earth to historical changes in ice loading. We solved the sea-level equation [*Farrell and Clark*, 1976] with calculations truncated at degree and order 256 representing a smoothing of the 5 km ice-sheet model output. The GIA model uses the methods described by *Kendall et al.* [2005], and includes rotational feedback [*Mitrovica et al.*, 2005]. The Earth is represented by a spherically symmetric, self-gravitating Maxwell body comprising an elastic lithosphere, and a uniform viscosity upper and lower mantle. Only ice-load changes in the AP were modeled in order to isolate the response to load changes in this region. However, the global sea-level equation was solved so that deformation due to changes in ocean loading in response to ice-mass change was included. The model was run for 160 years (1855-2015) with one year time steps and no change in ice thickness in the final five time steps, thus eliminating the elastic effects of a changing load from the calculated present-day uplift rate. It is important to note that ice-mass loss resulting indirectly from ice shelf break-up in the late 20th century, which would produce a large elastic signal [*Thomas et al.*, 2011], and an unknown viscous signal, has not been included in this study. We present GIA predictions for 2012.

The results of the GIA modeling are highly sensitive to the adopted Earth model (lithospheric thickness and mantle viscosity). It is widely reported [e.g., *Morelli and Danesi*, 2004] that East and West Antarctica have a markedly different Earth structure, with thick cratonic lithosphere and high-viscosity mantle dominating East Antarctica, and thinner lithosphere and lower mantle viscosity present in formerly tectonically active West Antarctica. *Ivins et al.* [2011] suggest that rheological parameters for the northern AP could be as low as 20-45 km for lithospheric thickness and 3-10 × 10^{19} Pa s for upper mantle viscosity. However, many GIA models use a single, and often comparatively strong, Earth model for the whole of Antarctica leading to incorrect predictions of present-day GIA uplift in the AP [*Thomas et al.*, 2011].

We investigated the effects that different input Earth models have on the predicted uplift rate, and found that the results are highly sensitive to upper mantle viscosity but less sensitive to lithospheric thickness and lower mantle viscosity. Within the GIA model, the range of values the Earth model can take are a lithospheric thickness of 46 km, 71 km, 96 km, or 120 km, upper mantle viscosity between 5×10^{19} Pa s and 5×10^{21} Pa s, and lower mantle viscosity between 1×10^{21} Pa s and 5×10^{22} Pa s. We present results for three different Earth models in Figure 3. In Figure 3a we use an Earth model appropriate for the northern AP with a lithospheric thickness of 46 km and upper mantle viscosity of 5×10^{19} Pa s, following the suggestion of *Ivins et al.* [2011]. In Figure 3b an Earth model which is likely to be representative of the Earth structure in the southern AP is used, with a thicker lithosphere of 71 km, and a stronger upper mantle viscosity of 1×10^{20} Pa s. For comparison, Figure 3c shows results using the preferred Earth model of *Whitehouse et al.* [2012b] for all Antarctica (lithospheric thickness of 120 km, upper mantle viscosity of 1×10^{21} Pa s). All models use the lower mantle viscosity from this last model (1×10^{22} Pa s).

Using the weakest Earth model, appropriate for the northern AP, the GIA model predicts between +0.4 and -7.0 mm/yr uplift, with the greatest subsidence predicted in the western AP (Figure 3a). In the northern Peninsula the maximum subsidence is around 3.5 mm/yr. A stronger Earth model, which is more appropriate for the southern AP, reduces the magnitude of the deformation to a peak subsidence of 3.2 mm/yr (Figure 3b). For an Earth model appropriate for all Antarctica, the peak subsidence is significantly reduced to 0.3 mm/yr (Figure 3c). The lower mantle viscosity has little effect on the results and sensitivity studies showed that decreasing the lower mantle viscosity by a factor of 10 to 1×10^{21} Pa s resulted in an increase in the magnitude of the peak subsidence rate by only 0.2 mm/yr, whilst increasing to 2×10^{22} Pa s made <0.01 mm/yr difference to the uplift rates.

5. Discussion

GIA-related subsidence of the magnitude presented here will have a dramatic effect on uplift rates, as recorded by GPS receivers. Such instruments have recently been deployed in the AP with the purpose of constraining models of GIA (see Figure 3c for known GPS locations), and interpretation of the data will need to consider the potential effect of recent ice-load changes on the observed velocities.

Thomas et al. [2011] report that GPS observations suggest low rates of GIA-related uplift in Antarctica, particularly along the AP where they do not exceed 2 mm/yr, and, in comparison, GIA models generally over-predict the signal. *Whitehouse et al.* [2012b] attempt to improve the fit between modeled GIA uplift and GPS-observed uplift by adding an arbitrary, uniform thickness of ice to the AP during the last 1000 years of an existing deglacial model [*Whitehouse et al.*, 2012a]. They find that this significantly improves the fit at all GPS sites on the AP but results in predicted subsidence on the eastern AP for which there is no clear observational evidence. Our study demonstrates that an east-west gradient in accumulation can generate a spatially variable GIA response that may help explain the observed low rates of GPS uplift in the AP. However, if our modeled ice-thickness changes were added to an existing deglaciation model for Antarctica, and combined with a strong Earth model that is representative of the majority of the continent, they would make very little difference to the results (e.g. Figure 3c with the preferred model of *Whitehouse et al.* [2012b] predicts < 1 mm/yr subsidence). In order to study the response to ice load changes in the AP in the context of a full Antarctic ice history, a 3-D Earth model would be required.

The effect of recent accumulation is, to date, unmodeled in recent ice-sheet reconstructions, including those used in GIA models. As a result, GIA corrections applied to Gravity Recovery and Climate Experiment (GRACE) data will be biased. To examine the effect on GRACE-determined rates of ice-mass change we calculated the geoid rate perturbation for each GIA model run and the resulting change in surface mass density, using the method described by *Wahr* *et al.* [1998] (equations 9 and 13). The surface mass density was then integrated over the area of the grounded ice sheet with an additional 100 km offshore buffer to obtain the total mass contribution for each GIA prediction. This provides realistic values for the correction to GRACE data as a ~100 km buffer would be included in the GRACE processing to capture any leakage from onshore ice-mass change. It is worth noting that the magnitude of the correction will be dependent upon the chosen width of the buffer. Over the AP, application of our GIA correction results in an increase in GRACE-determined rates of ice-mass change of +6.2 Gt/yr for the weakest Earth model, and +0.5 to +3.2 Gt/yr for stronger Earth models (Figure 3b-c). Previous mass balance estimates, derived using GRACE data, will therefore be biased low in the AP. Note that this correction only considers the GIA response to the recent accumulation increase described in our study, and will be additional to corrections for the long term GIA signal and the response to ice-mass loss from ice shelf break-up in the late 20th century.

This study has demonstrated the importance of Late Holocene ice loading in the modeling of GIA. This issue is relevant throughout Antarctica and GIA models will need to be revised as new data relating to this important time period are collected. This study is an improvement over previous attempts to model Late Holocene ice history; however, it highlights the clear need for more extensive datasets of past ice loading and uplift in the AP.

6. Conclusions

Accumulation reconstructions and ice-sheet modeling predict up to 45 m of ice-sheet thickening in the AP over the past 155 years, which may cause significant GIA-related subsidence. We note that high resolution modeling of accumulation may provide improvements to our ice load reconstruction in the future and the 5 km resolution of the ice sheet model may be a limitation for the complex topography of the northern AP. The modeled east-west gradient in accumulation produces a spatially varying GIA-uplift signal with the greatest subsidence predicted on the western AP. GIA model results are highly sensitive to the upper mantle viscosity of the adopted Earth model. The weakest Earth model tested, which is appropriate for the northern AP, predicts *subsidence* rates of up to 3.5 mm/yr in the northern AP. The Earth model which is likely to be appropriate for the southern AP predicts *subsidence* rates of up to 3.2 mm/yr in the southern AP. Current GIA models, which do not account for this loading, predict peak *uplift* rates of between 3 mm/yr [*Whitehouse et al.*, 2012b] and 15 mm/yr [*Ivins and James*, 2005] for the AP. If added to an existing ice-loading history, the extra ice loading modeled here may explain the low rates of GIA-related uplift observed in the AP from GPS measurements; however, due to the different Earth structure in West and East Antarctica, rigorous modeling would only be possible using a 3-D Earth model. GRACE-determined rates of ice-mass change are biased low for this region as a result of omitting this signal, and they may yet require further revision to reflect Late Holocene ice-load changes prior to 1850 [*Ivins et al.*, 2011]. However, the most important implication of our work is that accumulation-driven subsidence will significantly perturb GPS velocities which are used to validate or constrain models of GIA, and this highlights the need for more constraints on Late Holocene ice-sheet evolution to drive high resolution ice-sheet and GIA modeling.

Acknowledgements: Part of this work was supported by COST Action ES0701 "Improved constraints on models of Glacial Isostatic Adjustment". We thank Glenn Milne for providing the GIA model, Mark Tamisiea for supplying Earth model input, Michiel van den Broeke and Jan Lenaerts for providing SMB output from RACMO2.1/ANT, and Elizabeth Thomas for making ice core data available to us. We also thank Riccardo Riva and Anne Le Brocq for their valuable advice, and three anonymous reviewers for their helpful comments. G.A.N. is supported by a NERC PhD studentship. M.A.K. is supported by an RCUK Academic Fellowship.

References

Bevis, M., et al. (2009), Geodetic measurements of vertical crustal velocity in West Antarctica and the implications for ice mass balance, *Geochem. Geophys. Geosyst.*, *10*(10), Q10005, doi: 10.1029/2009gc002642.

Church, J. A., N. J. White, R. Coleman, K. Lambeck, and J. X. Mitrovica (2004), Estimates of the Regional Distribution of Sea Level Rise over the 1950–2000 Period, *Journal of Climate*, *17*(13), 2609-2625, doi: 10.1175/1520-0442(2004)017<2609:eotrdo>2.0.co;2.

Farrell, W. E., and J. A. Clark (1976), On Postglacial Sea Level, *Geophysical Journal of the Royal Astronomical Society*, *46*(3), 647-667, doi: 10.1111/j.1365-246X.1976.tb01252.x.

Ivins, E. R., and T. S. James (2005), Antarctic glacial isostatic adjustment: a new assessment, *Antarctic Science*, *17*(04), 541-553, doi: doi:10.1017/S0954102005002968.

Ivins, E. R., C. A. Raymond, and T. S. James (2000), The influence of 5000 year-old and younger glacial mass variability on present-day crustal rebound in the Antarctic Peninsula, *Earth, Planets and Space*, *52*(11), 1023-1029.

Ivins, E. R., M. M. Watkins, D.-N. Yuan, R. Dietrich, G. Casassa, and A. Rülke (2011), On-land ice loss and glacial isostatic adjustment at the Drake Passage: 2003–2009, *J. Geophys. Res.*, *116*(B2), B02403, doi: 10.1029/2010jb007607.

Kendall, R. A., J. X. Mitrovica, and G. A. Milne (2005), On post-glacial sea level – II. Numerical formulation and comparative results on spherically symmetric models, *Geophysical Journal International*, *161*(3), 679-706, doi: 10.1111/j.1365-246X.2005.02553.x.

Le Brocq, A. M., A. J. Payne, and A. Vieli (2010), An improved Antarctic dataset for high resolution numerical ice sheet models (ALBMAP v1), *Earth Syst. Sci. Data*, *2*(2), 247-260, doi: 10.5194/essd-2-247-2010.

Le Brocq, A. M., M. J. Bentley, A. Hubbard, C. J. Fogwill, D. E. Sugden, and P. L. Whitehouse (2011), Reconstructing the Last Glacial Maximum ice sheet in the Weddell Sea embayment, Antarctica, using numerical modelling constrained by field evidence, *Quaternary Science Reviews*, *30*(19-20), 2422-2432, doi: 10.1016/j.quascirev.2011.05.009.

Lenaerts, J. T. M., M. R. van den Broeke, W. J. van de Berg, E. van Meijgaard, and P. Kuipers Munneke (2012), A new, high-resolution surface mass balance map of Antarctica (1979-2010) based on regional atmospheric climate modeling, *Geophys. Res. Lett.*, *39*(4), L04501, doi: 10.1029/2011gl050713.

Miles, G. M., G. J. Marshall, J. R. McConnell, and A. J. Aristarain (2008), Recent accumulation variability and change on the Antarctic Peninsula from the ERA40 reanalysis, *International Journal of Climatology*, *28*(11), 1409-1422, doi: 10.1002/joc.1642.

Mitrovica, J. X., J. Wahr, I. Matsuyama, and A. Paulson (2005), The rotational stability of an ice-age earth, *Geophysical Journal International*, *161*(2), 491-506, doi: 10.1111/j.1365-246X.2005.02609.x.

Morelli, A., and S. Danesi (2004), Seismological imaging of the Antarctic continental lithosphere: a review, *Global and Planetary Change*, *42*(1-4), 155-165, doi: 10.1016/j.gloplacha.2003.12.005.

Mosley-Thompson, E. (1992), Paleoenvironmental conditions in Antarctica since A.D. 1500: Ice core evidence, in *Climate since A.D. 1500*, edited by R. S. Bradley and P. D. Jones, pp. 572-591, Routledge, London.

Peel, D. A. (1992), Ice core evidence from the Antarctic Peninsula region, in *Climate since A.D. 1500*, edited by R. S. Bradley and P. D. Jones, pp. 572-591, Routledge, London.

Rutt, I. C., M. Hagdorn, N. R. J. Hulton, and A. J. Payne (2009), The Glimmer community ice sheet model, *J. Geophys. Res.*, *114*(F2), F02004, doi: 10.1029/2008jf001015.

Thomas, E. R., G. J. Marshall, and J. R. McConnell (2008), A doubling in snow accumulation in the western Antarctic Peninsula since 1850, *Geophys. Res. Lett.*, *35*(1), L01706, doi: 10.1029/2007gl032529.

Thomas, I. D., et al. (2011), Widespread low rates of Antarctic glacial isostatic adjustment revealed by GPS observations, *Geophys. Res. Lett.*, *38*(22), L22302, doi: 10.1029/2011gl049277.

Wahr, J., M. Molenaar, and F. Bryan (1998), Time variability of the Earth's gravity field: Hydrological and oceanic effects and their possible detection using GRACE, *J. Geophys. Res.*, *103*(B12), 30205-30229, doi: 10.1029/98jb02844.

Whitehouse, P. L., M. J. Bentley, and A. M. Le Brocq (2012a), A deglacial model for Antarctica: geological constraints and glaciological modelling as a basis for a new model of Antarctic glacial isostatic adjustment, *Quaternary Science Reviews*, *32*, 1-24, doi: 10.1016/j.quascirev.2011.11.016.

Whitehouse, P. L., M. J. Bentley, G. A. Milne, M. A. King, and I. D. Thomas (2012b), A new glacial isostatic adjustment model for Antarctica: calibrated and tested using observations of relative sea-level change and present-day uplift rates, *Geophysical Journal International*, doi: 10.1111/j.1365-246X.2012.05557.x.

Figure Captions

Figure 1: Annual accumulation in meters water equivalent (m_{weq}) derived from ice core records (dark solid lines) and extrapolated to 2010 (light solid lines). EOF-reconstructed accumulation time series are shown for each location using data from all ice cores (a, dotted lines), and data from all ice cores except the one being reconstructed (b, dashed lines). Ice-core locations are shown in the inset. Ice core records reproduced from *Mosley-Thompson* [1992], *Peel* [1992], and *Thomas et al.* [2008].

Figure 2: (a) Ice-sheet model output showing net ice thickness change between 1855 and 2010; (b) Sum of the reconstructed accumulation history between 1855 and 2010; (c) Effect of ice flow, i.e. (b) minus (a). Ice core locations are shown as red circles. Note that a different color scale is used in each plot. The southern boundary of the ice sheet model domain is shown as a black dotted line. Axes are Antarctic Polar Stereographic X, Y (km).

Figure 3: Present-day GIA uplift rates for Earth models (lithospheric thickness h, upper mantle viscosity η_{UM} and lower mantle viscosity η_{LM}): (a) appropriate for the northern AP; (b) appropriate for the southern AP; and, (c) *Whitehouse et al.* [2012b] preferred Earth model. GPS locations are shown as pink circles in (c). Axes are Antarctic Polar Stereographic X, Y (km).

a.

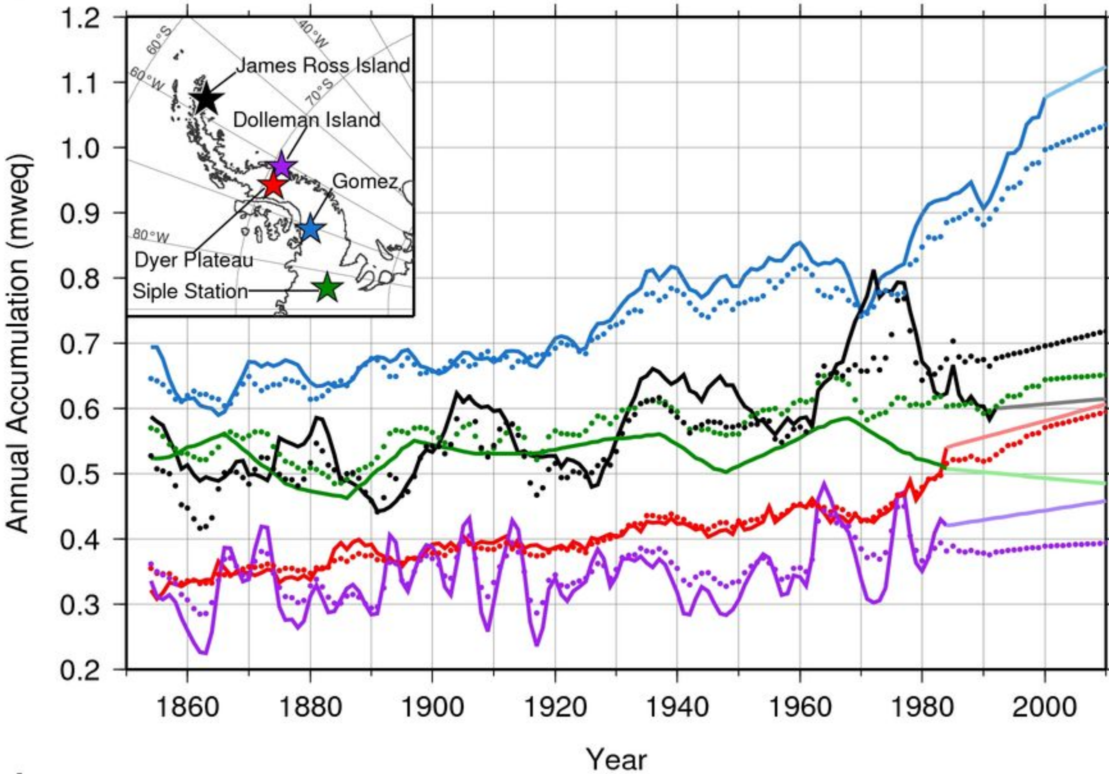

James Ross Island
Dolleman Island
Gomez
Dyer Plateau
Siple Station
60°S
40°W
60°W
70°S
80°W
Annual Accumulation (mweq)
Year

b.

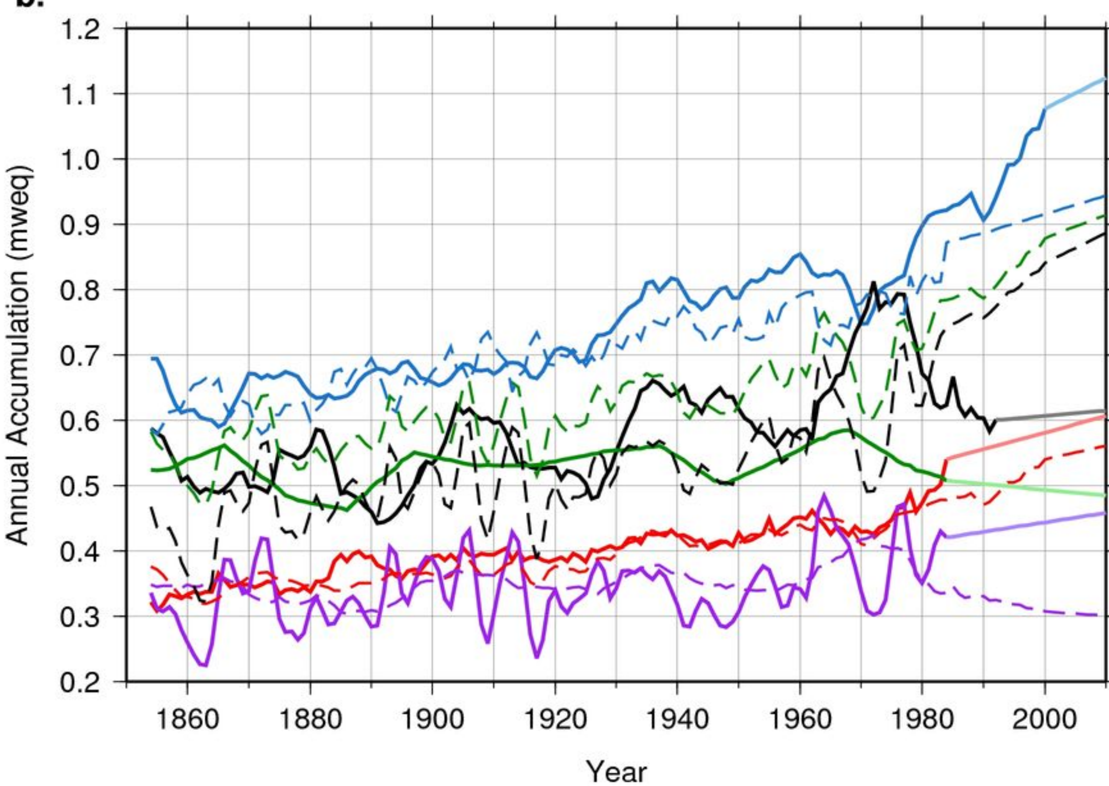

Annual Accumulation (mweq)
Year

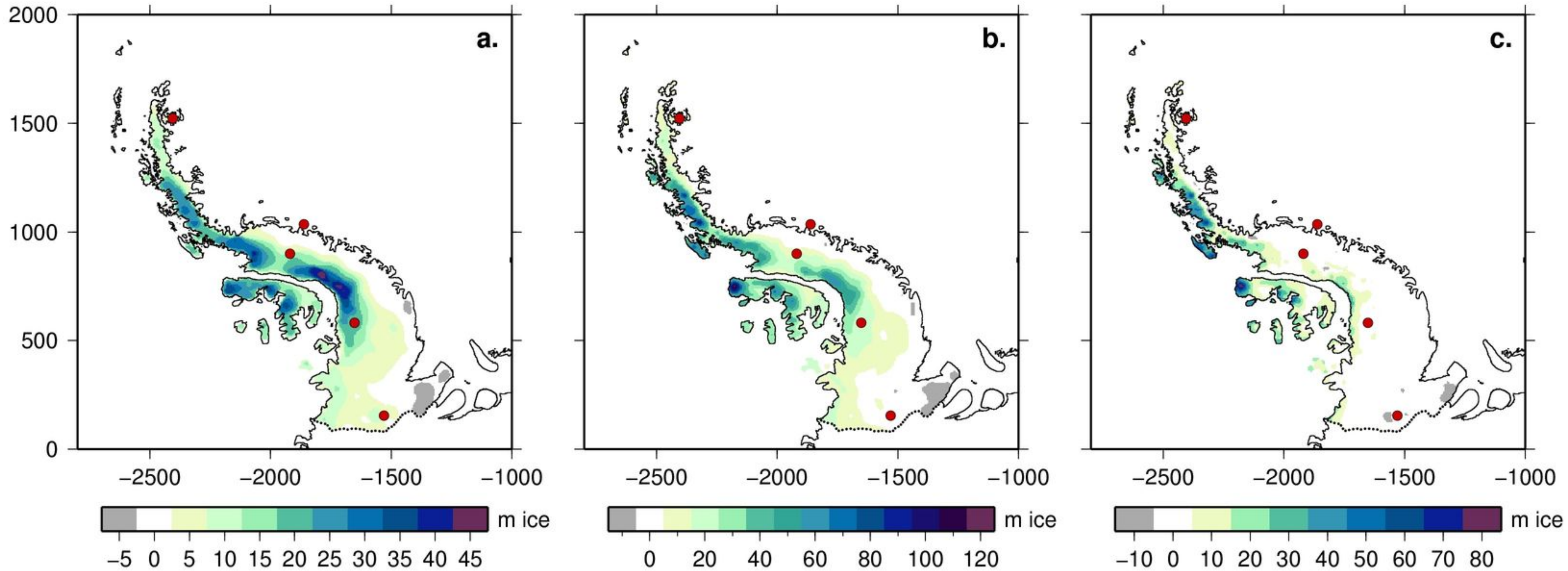
a.
b.
c.
2000
1500
1000
500
0
−2500
−2000
−1500
−1000
−5 0 5 10 15 20 25 30 35 40 45
m ice
0 20 40 60 80 100 120
m ice
−10 0 10 20 30 40 50 60 70 80
m ice

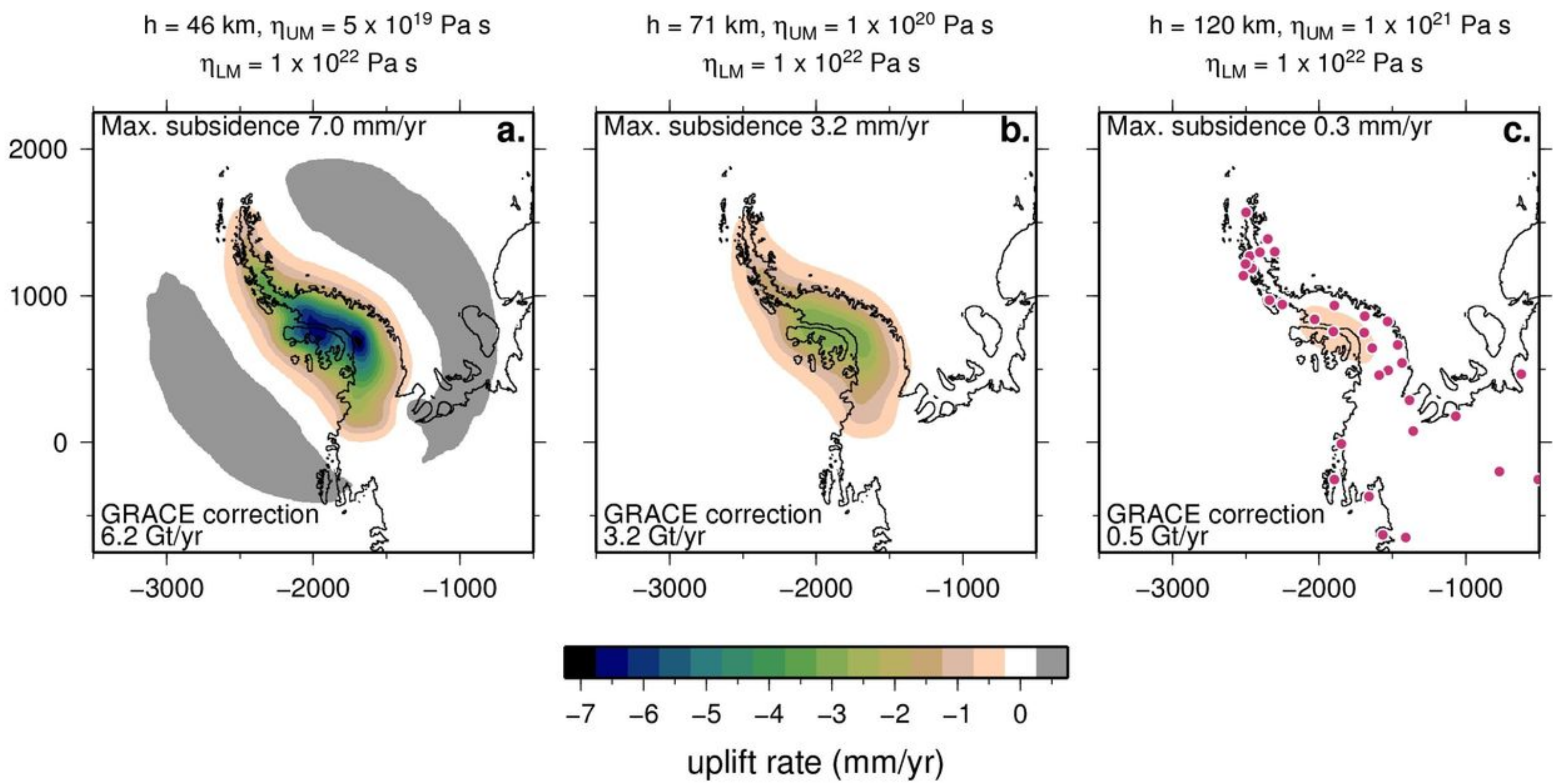

h = 46 km, η_{UM} = 5 x 10^{19} Pa s
η_{LM} = 1 x 10^{22} Pa s
h = 71 km, η_{UM} = 1 x 10^{20} Pa s
η_{LM} = 1 x 10^{22} Pa s
h = 120 km, η_{UM} = 1 x 10^{21} Pa s
η_{LM} = 1 x 10^{22} Pa s
Max. subsidence 7.0 mm/yr
a.
GRACE correction
6.2 Gt/yr
Max. subsidence 3.2 mm/yr
b.
GRACE correction
3.2 Gt/yr
Max. subsidence 0.3 mm/yr
c.
GRACE correction
0.5 Gt/yr
2000
1000
0
−3000
−2000
−1000
−7 −6 −5 −4 −3 −2 −1 0
uplift rate (mm/yr)